Electrochromics by Intramolecular Redox Switching of Single Bonds[‡]

Siegfried Hünig,*[a] Sven Aldenkortt,[a] Peter Bäuerle,[b] Christoph A. Briehn,[b] Michael Schäferling,[b] Igor F. Perepichka,[c] Dietmar Stalke,[d] and Bernhard Walfort[d]

Dedicated to Professor Manfred Christl on the occasion of his 60th birthday

Keywords: Cyanines / Cyclic voltammetry / Electrochromics / Spectroelectrochemistry

Compounds of the general structure presented in Scheme 1 are proposed as electrochromic systems (ESs) in which reversible electron transfer is associated with breaking or forming of single bonds. In contrast to classical ESs, both redox states represent closed-shell systems. Whereas type OL/CS (*O*pen form – *L*ong-wavelength absorption/*C*losed form – *S*hort-wavelength absorption) has already been demonstrated, this paper presents examples of the OS/CL type, in which the long-wavelength absorption is displayed by the ring-closed form. Bis(azines) **RED-8**, **RED-13**, **RED-16**, and **RED-17**, as well as the bis(amines) **RED-22**, **RED-23**, and **RED-24** were prepared and characterized by their cyclic voltammograms (CV) and spectroelectrograms (SE). Except for the case of **RED-24**, the reversible overall transfer of two electrons is connected to switching of a single C–C or N–N bond. This reaction is not restricted to an entropically favorable transannular reaction (**OX-8**$^{2+}$, **OX-16**$^{2+}$, and **OX-17**$^{2+}$) but also occurs with the formation of five- (**OX-13**$^{2+}$ and **OX-23**$^{2+}$) and certain six-membered rings (**OX-22**$^{2+}$). These results suggest that the OS/CL general structure type should allow broad variation both in redox potentials and in ranges of color, similarly to the OL/CS type.

Introduction

We have recently described a new general principle for electrochromics through redox switching of single bonds according to Scheme 1.[1] In Part I of this series we dealt with the OL/CS type, in which the *O*pen form displays *L*ong-wavelength absorption and the *C*losed one *S*hort-wavelength absorption. The chromophores were mono- and trimethine cyanines and styryl dyes in which two units were linked throughout by a saturated tether at one of their methine groups.

We now report on examples representing the OS/CL type, as in Scheme 1. Here, the *O*pen form displays *S*hort-wavelength absorption and the *C*losed one *L*ong-wavelength absorption. Again, this report is restricted to the syntheses of the starting materials and their characterization by cyclic voltammetry (CV) and spectroelectrochemistry (SE), together with X-ray structure analysis of and semiempirical calculations on **RED-8** (and its oxidation products). The suggested structures of the products are based only on these data and analogies from the literature.

Redox switching of single bonds corresponding to OS/CL is well documented in the literature, but not with cyanine, merocyanine, or oxonol end groups in the closed form and thus lacking light absorption in the visible region. These systems are listed in Table 1. Compound **4**, with two dimethylamino groups in the 1,1-position, has been smoothly oxidized by silver ions. Reduction of the corresponding dication back to the starting material, although not previously reported, should proceed without difficulties. Very recently, system **5**, meeting all requirements of the OS/CL type, has been described.[2–6]

[‡] The Second Type, 2. Part 1: Ref.[1]

[a] Institut für Organische Chemie der Universität Würzburg, Am Hubland, 97074 Würzburg, Germany
Fax: (internat.) + 49-(0)931/888-4606
E-mail: huenig@chemie.uni-wuerzburg.de
[b] Abteilung Organische Chemie II der Universität Ulm, Albert-Einstein-Allee 11, 89081 Ulm, Germany
Fax: (internat.) + 49-(0)731/502-2840
E-mail: peter.baeuerle@chemie.uni-ulm.de
[c] L. M. Litvinenko Institute of Physical Organic and Coal Chemistry, National Academy of Sciences
R. Luxemburg Street 70, Donetsk 83114, Ukraine
Fax: (internat.) + 380-622/558524
E-mail: i perepichka@yahoo.com
[d] Institut für Anorganische Chemie der Universität Würzburg, Am Hubland, 97074 Würzburg, Germany
Fax: (internat.) + 49-(0)931/888-4619
E-mail: dstalke@chemie.uni-wuerzburg.de

Supporting information for this article is available on the WWW under http://www.eurjoc.com or from the author.

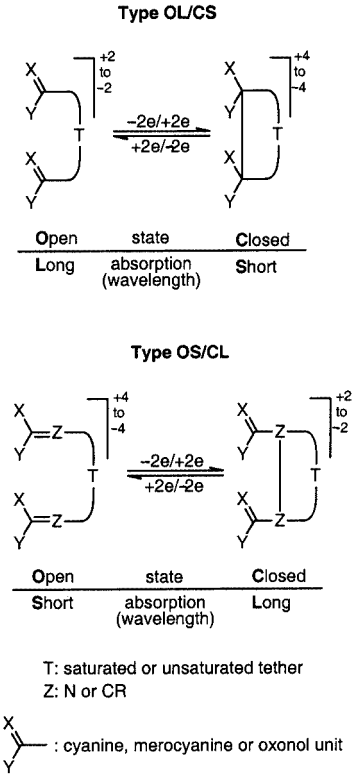

Scheme 1. General structures for electrochromics by single bond redox switching

Table 1. Known systems with redox single bond switching similar to type OS/CL

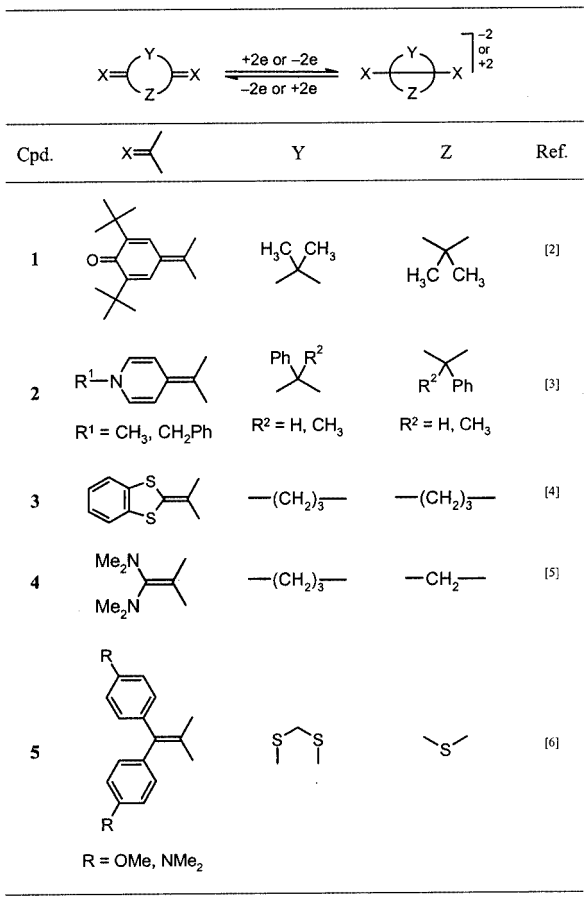

Results and Discussion

Azines from 4,4′-Bis(dimethylamino)benzophenone Hydrazone 6 and Diketones

Bis(azine) RED-8

According to the pattern shown in Scheme 1, we started out with redox system **RED-8**, in which the potential chromophores are linked to a cyclic core. Hydrazone **6**[7] smoothly reacted with cyclooctane-1,5-dione (**7**) to afford the pale yellow bis(azine) **RED-8** in 73% yield (Scheme 2).

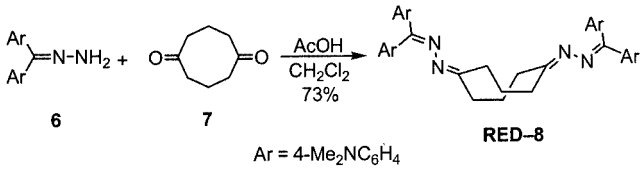

Scheme 2. Synthesis of bis(azine) **RED-8**

The anticipated structure of **RED-8** was confirmed by X-ray analysis. However, unexpectedly, **RED-8** prefers a boat conformation, at least in the crystal lattice (Figure 1). In addition, one 4-dimethylamino ring in each diaryl ketazine moiety is strongly twisted out of plane and so is not available for conjugational stabilization.

PM3 calculations on **RED-8** indicated that the boat conformations, which could be represented by three conformers with different orientations of the azine chains (see Supporting Information), were close to the chair-like conformation in energies. The most stable boat-like conformation was of nearly the same PM3 energy as the chair-like conformation (Table 2). In all boat conformations, the 4-(dimethylamino)phenyl moieties were strongly twisted out of plane of the azine fragment, which is in agreement with the X-ray data.

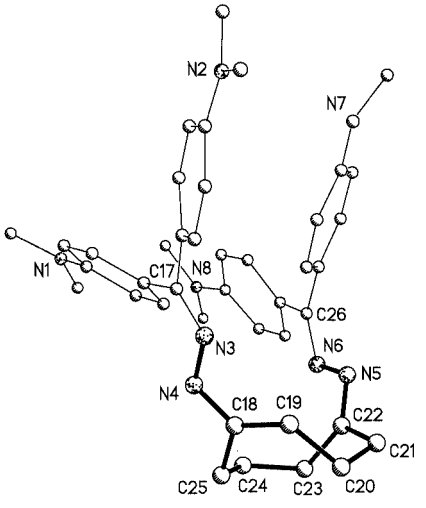

Figure 1. X-ray structure of **RED-8**

Table 2. Energies for PM3- and AM1-optimized geometries of bicyclic dications **OX-8^{2+}** (5/5), **OX-8^{2+}** (7/7), and **OX-8^{2+}** (9/9), and dications **OX-8^{2+}** (8) and **OX-8$^{2+\cdot}$** (8)

Compound	Method	E_h [Hartree][a]	$\Delta H_f°$ [kcal/mol]	$\Delta\Delta H_f°$ (c/o) [kcal/mol]
RED-8 (boat)	RHF/PM3	−259.919547	173.27	(0)
RED-8 (chair)	RHF/PM3	−259.919446	173.33	+0.06
OX-8^{2+} (8)	RHF/PM3	−259.281282	573.79	(0)
OX-8^{2+} (5/5)	RHF/PM3	−259.367730	519.55	−54.24
OX-8^{2+} (7/7)	RHF/PM3	−259.294801	565.31	−8.48
OX-8^{2+} (9/9)	RHF/PM3	−259.284781	571.60	−2.19
OX-8$^{2+\cdot}$ (8)	UHF/PM3	−259.356762	526.43	(0)
OX-8^{2+} (5/5)	UHF/PM3	−259.370628	517.73	−3.36
OX-8^{2+} (8)	RHF/AM1	−283.982786	610.64	(0)
OX-8^{2+} (5/5)	RHF/AM1	−284.054106	565.88	−44.76
OX-8^{2+} (7/7)	RHF/AM1	−283.968579	619.55	+8.91
OX-8^{2+} (9/9)	RHF/AM1	−283.961043	624.28	+14.24
OX-8$^{2+\cdot}$ (8)	UHF/AM1	−284.053796	566.07	(0)
OX-8^{2+} (5/5)	RHF/AM1	−284.054106	565.88	+0.19

[a] E_h is the total energy of the molecule, $\Delta H_f°$ is the heat of formation, and $\Delta\Delta H_f°$ is the difference in the heats of formation between the structure with no transannular bond [**OX-8^{2+}** (8) or **OX-8$^{2+\cdot}$** (8)] and the bicyclic structures (or between the boat and the chair conformations of **RED-8**).

The differences in the ordering of the aryl groups were lost in solution on the ^{1}H NMR timescale. Surprisingly, however, a second set of similar signals (ca. 10%) arose in a freshly prepared solution of **RED-8** (in [D$_3$]MeCN). After 1 d, the two sets of signals had reached a ratio of 1:1, which was hardly affected on heating to 90 °C. Possibly, the conformation of **RED-8**, as delivered from the crystal lattice (cf. Figure 1), partly changes into another of similar energy, as suggested by the PM3 calculations. More than one set of signals have also been observed with some other diarylketazines.[8,9] Figure 2 provides information about the electrochemical behavior of **RED-8** and the structures of the possible oxidation products. The CV of **RED-8** remained unchanged on multiscanning, indicating an overall reversible

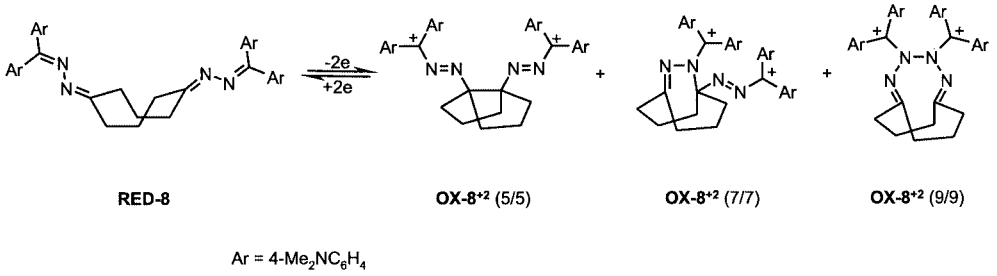

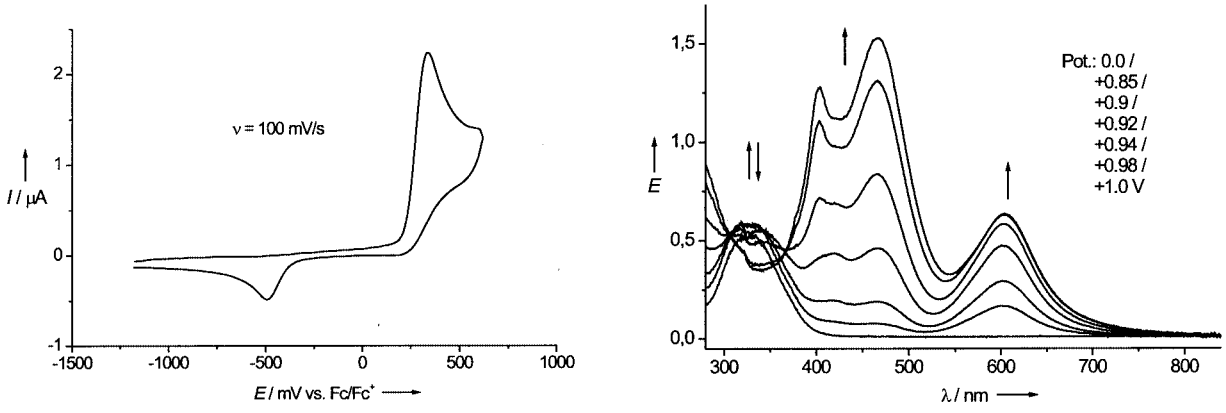

Figure 2. Cyclic voltammogram (CV) and spectroelectrogram (SE) of **RED-8** in acetonitrile

chemical reaction. The large difference (ΔE = 826 mV) between the oxidation and reduction peak, however, ruled out reversible electron transfer only and pointed to pronounced structural changes.[10] In the SE of **RED-8**, three absorption maxima were reversibly and concurrently built up, at $\lambda \approx$ 400 nm, 460 nm, and 610 nm.

In principle, the three maxima might be attributable to the three possible products **OX-8**$^{2+}$ (5/5), **OX-8**$^{2+}$ (7/7), and **OX-8**$^{2+}$ (9/9). The transannular reaction to afford **OX-8**$^{2+}$ (5/5) seems to be most likely, with a bicyclic system with two five-membered rings being created as the isomer of lowest energy (vide infra). In accordance with this view, the bis(hydrazone) **9** smoothly forms the bicyclic bis(azo) compound **10** (5/5) on oxidation (Scheme 3).[11]

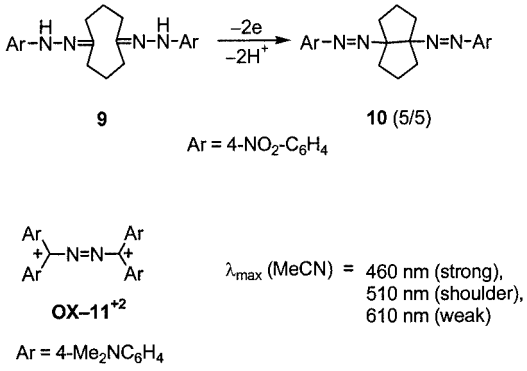

Scheme 3. Oxidation of bis(hydrazone) **9**

The absorption bands of **OX-8**$^{2+}$ at λ = 400, 460, and 610 nm correlated with those of the dye cation **OX-11**$^{2+}$ (obtained by SE).[12] Again, the longest wavelength absorption that could be attributable to Michler's hydrol type

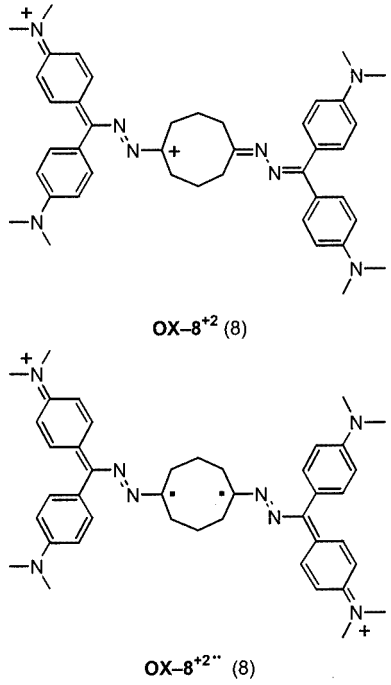

Figure 3. Possible structures of dications derived from bis(azine) **RED-8**: dications **OX-8**$^{2+}$ (8) without a transannular bond; bicyclic dications **OX-8**$^{2+}$ (5/5), **OX-8**$^{2+}$ (7/7), and **OX-8**$^{2+}$ (9/9) are shown in Figure 2

showed rather low intensity (cf. Scheme 3). By this interpretation, not only the expected absorption at λ = 610 nm (Michler's hydrol blue type) but also those at λ = 400 and 460 nm should belong to the chromophore of **OX-8**$^{2+}$ (5/5), although isomers **OX-8**$^{2+}$ (7/7) and **OX-8**$^{2+}$ (9/9) would be expected to absorb in the same range. However, the new

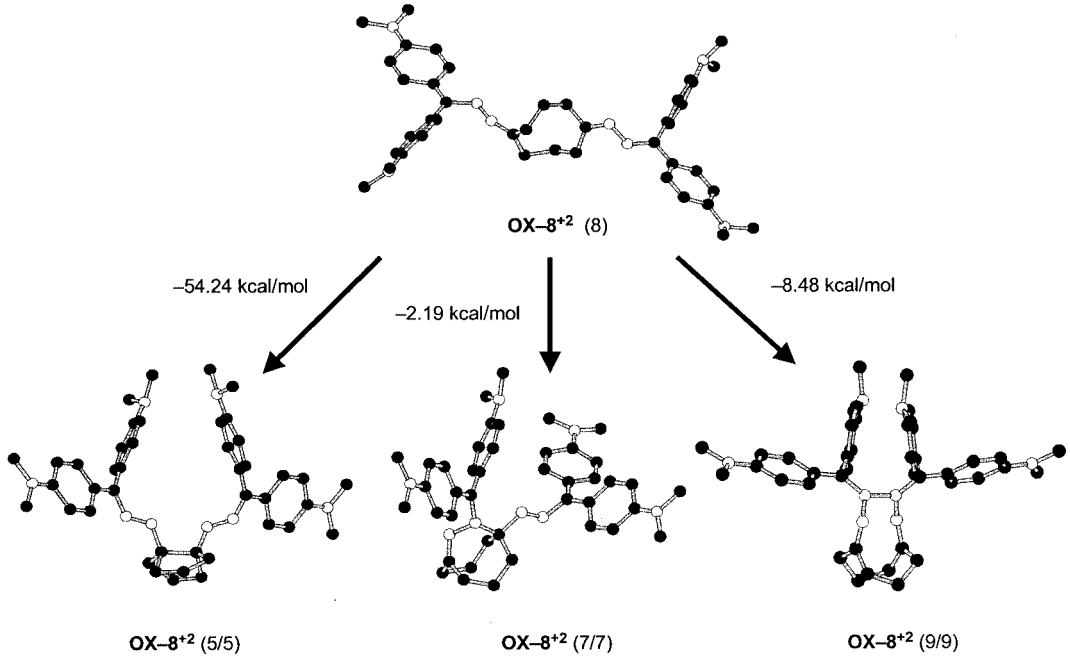

Figure 4. PM3-optimized geometries of the hypothetical oxidation product **OX-8**$^{2+}$ (8) and the three possible transannular products **OX-8**$^{2+}$ (5/5), **OX-8**$^{2+}$ (7/7), and **OX-8**$^{2+}$ (9/9) together with their differences in energy compared to **OX-8**$^{2+}$ (8); filled circles are carbon atoms, open circles are nitrogen atoms, hydrogen atoms are omitted for clarity

absorption bands did not develop uniformly with progressing oxidation of **RED-8**. Initially, the 610 nm band was preferred, but was later surmounted by the shorter-wavelength bands. Consequently, the two isosbestic points were not as sharp as would be expected for a simple equilibrium between two components. The data in Figure 2 do not allow a very sound analysis of this phenomenon. Possibly, the different conformations of **RED-8** − assuming slightly different oxidation potentials − are involved.

The arguments in favor of **OX-8^{2+}** (5/5) were supported by PM3-calculated heats of formation for the three possible isomeric ring-closed oxidation products of **RED-8** (Table 2). From general considerations, these cyclic structures should be preferred over the open structure **OX-8^{2+}** (8), which would be unfavorable because of the closed-shell state of **OX-8^{2+}** (8). The charge delocalization is unsymmetrical, with one positive charge on the dimethylammonium fragment but another one on a carbon atom; the structure should otherwise have a diradical character [**OX-8$^{2+\cdot\cdot}$** (8)] (Figure 3).

As may be judged from Figure 4, **OX-8^{2+}** (5/5) should definitely be preferred (−54 kcal/mol) since **OX-8^{2+}** (7/7) was higher in energy by 52 kcal/mol and **OX-8^{2+}** (9/9) still by 46 kcal/mol. Interestingly, as with **OX-11^{2+}**,[12] no nearly coplanar arrangement of the cationic "Michler's hydrol blue moiety" was found. One 4-(dimethylamino)phenyl group in these moieties seems to be lower in energy when twisted out of plane. This may explain the strong absorptions of **OX-8^{2+}** (5/5) at wavelengths shorter than ca. 610 nm. These arguments were backed by PM3-calculated geometries for the three possible isomeric ring-closed oxidation products of **RED-8**, and the energies were compared to that of the hypothetical dication **OX-8^{2+}** (8) without a transannular bond (Figures 3 and 4). When the restricted Hartree−Fock formalism was applied for the closed-shell PM3 optimization of the geometries, all three bicyclic structures [**OX-8^{2+}** (5/5), **OX-8^{2+}** (7/7), and **OX-8^{2+}** (9/9)] were found to be more stable than the open structure **OX-8^{2+}** (8) without a transannular bond (Table 2).

To take account of the alternative possibility of the existence of the open form of the dication as a diradical, we performed a UHF/PM3 calculation for **OX-8$^{2+\cdot\cdot}$** (8) in a triplet state and compared the energy of that with the UHF/PM3 singlet state for the bicyclic structure **OX-8^{2+}** (5/5). Again the cyclic structure was energetically preferred (by 3.36 kcal/mol). Although, as follows from gas phase calculations, the difference in energies between **OX-8^{2+}** (5/5) and **OX-8$^{2+\cdot\cdot}$** (8) was drastically reduced, the stabilization of **OX-8^{2+}** (5/5) in solution should be expected to be more pronounced than that of the diradical dication **OX-8$^{2+\cdot\cdot}$** (8). Moreover, experimentally the two-electron oxidation of **RED-8** resulted in a species with long-wavelength absorbance at around 600 nm, in good agreement with other, similar systems producing closed-shell systems with cyanine end groups on oxidation.[12,18,19] In contrast, when radical cation species are formed on oxidation in such a system the longest wavelength absorption is observed at substantially lower energies, in the near IR region.[12,19]

RHF/AM1 calculations produced geometries (see Supporting Information) and energy differences between the three possible oxidation products similar to those calculated by RHF/PM3 (Table 2). However, there were some differences from PM3 energies. Whereas **OX-8^{2+}** (5/5) was again the most stable isomer, showing a preference over the open structure **OX-8^{2+}** (8) of ca. 45 kcal/mol, two other bicyclic cations, **OX-8^{2+}** (7/7) and **OX-8^{2+}** (9/9), were found to be less stable than **OX-8^{2+}** (8) by ca. 9 kcal/mol and 14 kcal/mol, respectively.

Bis(azine) RED-13

The reversible redox system **RED-8** was designed to allow transannular bond formation in a rather rigid eight-membered ring. The question arose of whether the observed single bond switching would also be possible in an open-chain derivative with the redox-active groups also in the 1,5-position. Therefore, bis(azine) **RED-13** was synthesized from hydrazone **6** and heptane-2,6-dione (**12**), as a yellow powder in 70% yield (Scheme 4). Figure 5 demonstrates that **RED-13** indeed displayed redox properties similar to those of **RED-8**. The CV showed chemical, but not electrochemical, reversibility.

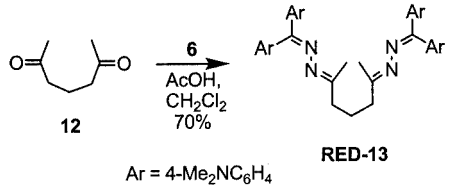

Scheme 4. Synthesis of bis(azine) **RED-13**

Both peak intensities increased with the scan rate, since more electroactive material was caught in the diffusion layer. However, the very small oxidation and reduction peaks (around 0 mV and −700 mV, respectively) accompanying the large ones are difficult to interpret (isomers?, adsorption?, stepwise electron transfer?). In the SE, the different absorption bands developed on progressing oxidation in a manner similar to those in **RED-8**. However, the isosbestic point was fairly sharp. The reason for this behavior should be similar to those discussed above. Analogously to **RED-8**, the three possible oxidation products **OX-13^{2+}** (5), **OX-13^{2+}** (7), and **OX-13^{2+}** (9) are given; of these the isomer with the five-membered ring would be supposed to be the most likely one.

Bis(azines) RED-16 and RED-17

In sharp contrast to the highly flexible heptane-2,6-dione (**12**, on which **RED-13** is based), the rigid cage diones **14** and **15**[13] were employed to synthesize bis(azines) **RED-16** and **RED-17** as shown in Scheme 5.

In **14** and **15**, the two carbonyl groups are held in nearly parallel positions; the distance between the two carbon atoms (for **14**, **15**: d = 260 pm[14]), however, is too large to form a single bond on reduction, and so no pinacol formation can be observed.[15] In other words, these carbon atoms

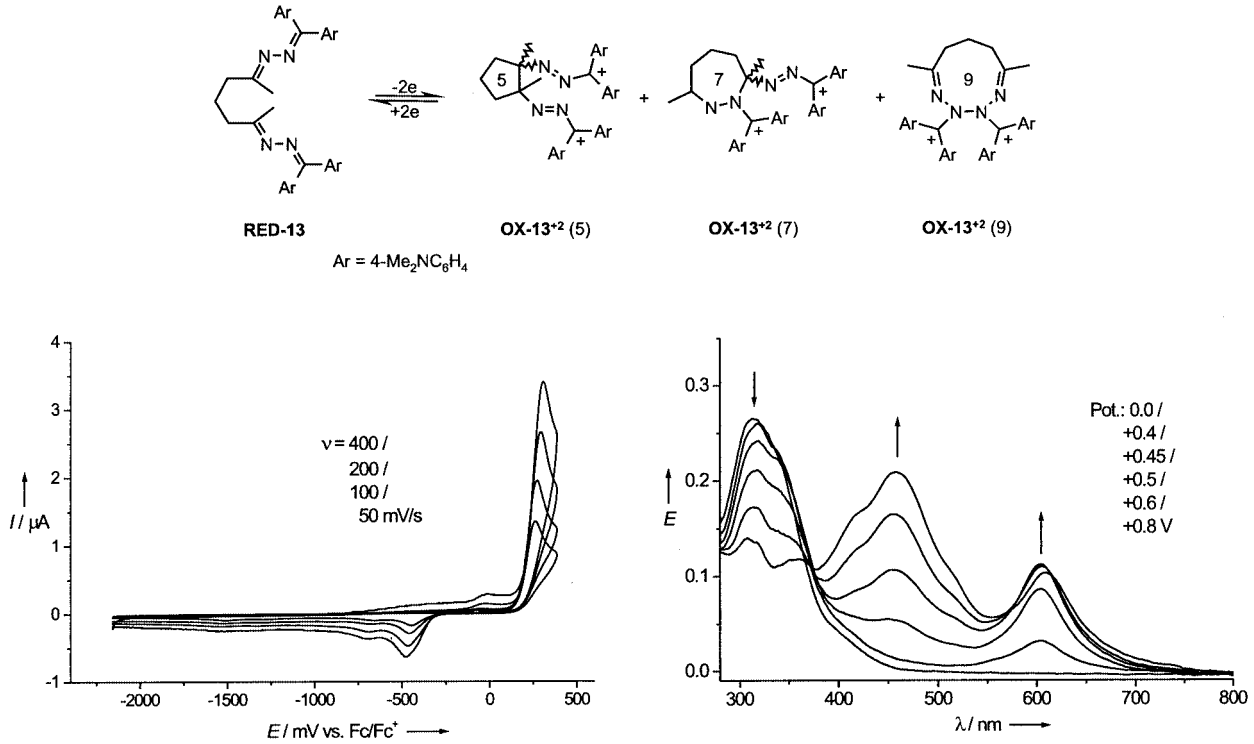

Figure 5. Cyclic voltammogram (CV) and spectroelectrogram (SE) of **RED-13** in benzonitrile

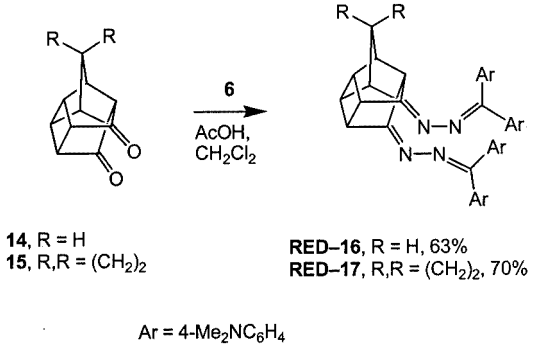

Scheme 5. Syntheses of bis(azines) **RED-16** and **RED-17**

cannot be involved if a new single bond is formed on oxidation of **RED-16** and **RED-17**. The electrochemical properties of **RED-17** duplicated those of **RED-16**, and so only those of the latter are presented in Figure 6.

The CV of **RED-16** shown in Figure 6 displays two close oxidation peaks. Two oxidation peaks were also observed in the CVs of **RED-8** and **RED-13**. These peaks were better separated, already allowing scan reversal after the first oxidation peaks (Figures 2 and 5), indicating that the second peak was not involved in the redox process described. We therefore view the second oxidation and the first small reduction peak in Figure 6 as indicative of a further oxidation of **OX-16**$^{2+}$. Between these oxidation peaks, the other two rather small oxidation signals may be associated with the hydrazone system formed (cf. **RED-22**, Figure 7). With increasing scan rate the CV developed a small reduction peak at ca. 330 mV, which may indicate some reversible electron transfer. Even the reductive ring-opening might partly occur stepwise, since besides the reduction peak at $E = -525$ mV, another, very broad one, became visible at $E = -1545$ mV. Both CV and SE of **RED-16** indicated an overall chemically reversible process between two components, but no reversible electron transfer. In the SE, only a faint absorption was to be seen at ca. 600 nm; the main absorption bands were found at ca. 400 nm, 430 nm, and 455 nm. Therefore, as anticipated, the chromophoric system did not compare with that of **OX-8**$^{2+}$. Rather, the new single bond was most probably formed between the two nitrogen atoms, according to **OX-16**$^{2+}$. The orange color would now correspond to that of protonated imines derived from Michler's ketone (auramine type).

Bis(imines) from 4,4′-Bis(dimethylamino)benzophenone (Michler's Ketone)

On the assumption of probable N−N bond formation in **OX-16**$^{2+}$ and **OX-17**$^{2+}$, bifunctional imines with potential cyanine-type end groups should undergo similar redox switching of a single bond. As already mentioned, the longest-wavelength absorption would then be expected in the range of 420−500 nm. Model compounds **RED-22**, **RED-23**, and **RED-24** were easily prepared from salt **18**[16] and the appropriate diamines **19**−**21** according to the synthesis illustrated in Scheme 6.

Bis(imine) RED-22

The bis(imine) **RED-22**, derived from 2,2′-diaminobiphenyl (**19**), showed well-behaved reversible redox properties demonstrated by multi-sweep CVs and by its SE. As shown in Figure 7, the oxidized product absorbed within the expected spectral range.

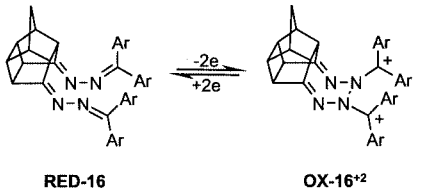

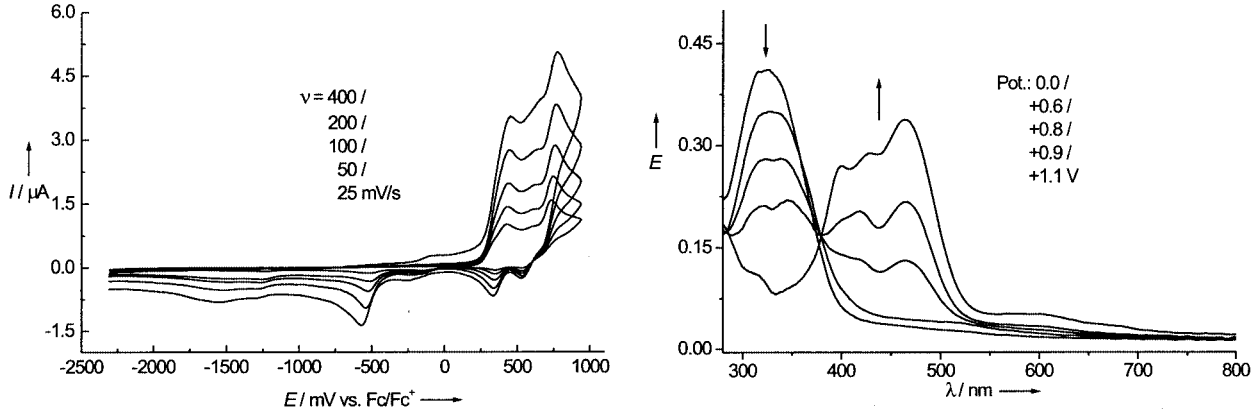

Figure 6. Cyclic voltammogram (CV) and spectroelectrogram (SE) of **RED-16** in benzonitrile

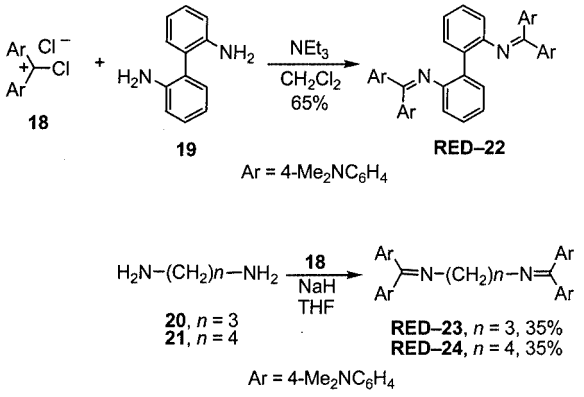

Scheme 6. Syntheses of bis-imines **RED-22**, **RED-23**, and **RED-24**

The CV of **RED-22** showed the same large separation between the first oxidation peak and the reduction peak, typical of an irreversible electron transfer. Thus, for **OX-22^{2+}** the cyclic structure of Figure 7 became plausible. The other oxidation peaks of the CV were less clear (vide supra). Two of them might be due to a diarylhydrazine substructure, since aryl-substituted hydrazines are known to be oxidized to radical cations and dications.[17]

Bis(imines) RED-23 and RED-24

In **RED-22** the bis(imine) moiety consists of two rigid parts that may flip only along the biphenyl axis and therefore provide good opportunities for N−N bond formation on oxidation. The question therefore arose of whether this new bond would also smoothly be closed if the two imino groups were linked by a highly flexible tether. Thus, **RED-23** and **RED-24**, with three and four methylene groups as connective units, were synthesized. Indeed, both CV and SE characterized **RED-23** as a well-behaved member of the general type OS/CL. Its electrochemical and spectral properties resembled those of **RED-22**. The pyrazolidine structure of **OX-23^{2+}** therefore seemed most likely for the oxidation product (Figure 8).

In contrast, **RED-24**, which had been anticipated to form a six-membered ring on oxidation, obviously preferred side reactions. CVs of **RED-24** in acetonitrile were troubled by strong adsorptions at the platinum electrode. This behavior could be minimized if benzonitrile was used as solvent, but the overall chemical reversibility was still not sufficient. Probably a too strong decrease in entropy prevented the smooth formation of a six-membered ring **OX-24^{2+}**, in sharp contrast to the less flexible six-membered ring in **OX-22^{2+}**.

Conclusion

Scheme 1 suggests two variants for electrochromic systems involving intramolecular reversible redox switching of single bonds. Type OL/CS has recently been shown to be applicable by a series of examples.[1] This paper clearly demonstrates that the same is true for type OS/CL, in which the closed form provides the long-wavelength absorbing product. Both C−C (**OX-8^{2+}** and **OX-13^{2+}**) and N−N (**OX-16^{2+}**, **OX-22^{2+}**, and **OX-23^{2+}**) bond formation can be achieved. This oxidative ring-closure is not restricted to entropically favorable transannular reactions (**OX-8^{2+}**, **OX-16^{2+}**, and **OX-17^{2+}**), but also works with the formation of monocyclic rings (**OX-13^{2+}**, **OX-22^{2+}**, and **OX-23^{2+}**) if a

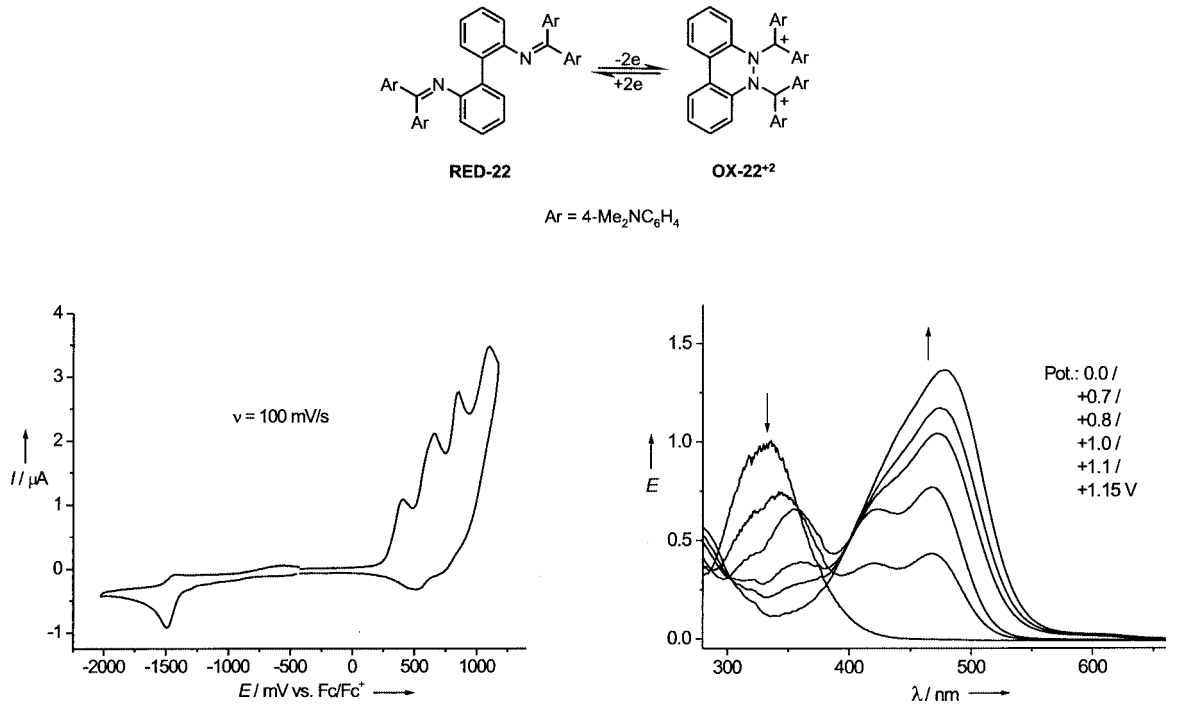

Figure 7. Cyclic voltammogram (CV) and spectroelectrogram (SE) of **RED-22** in benzonitrile

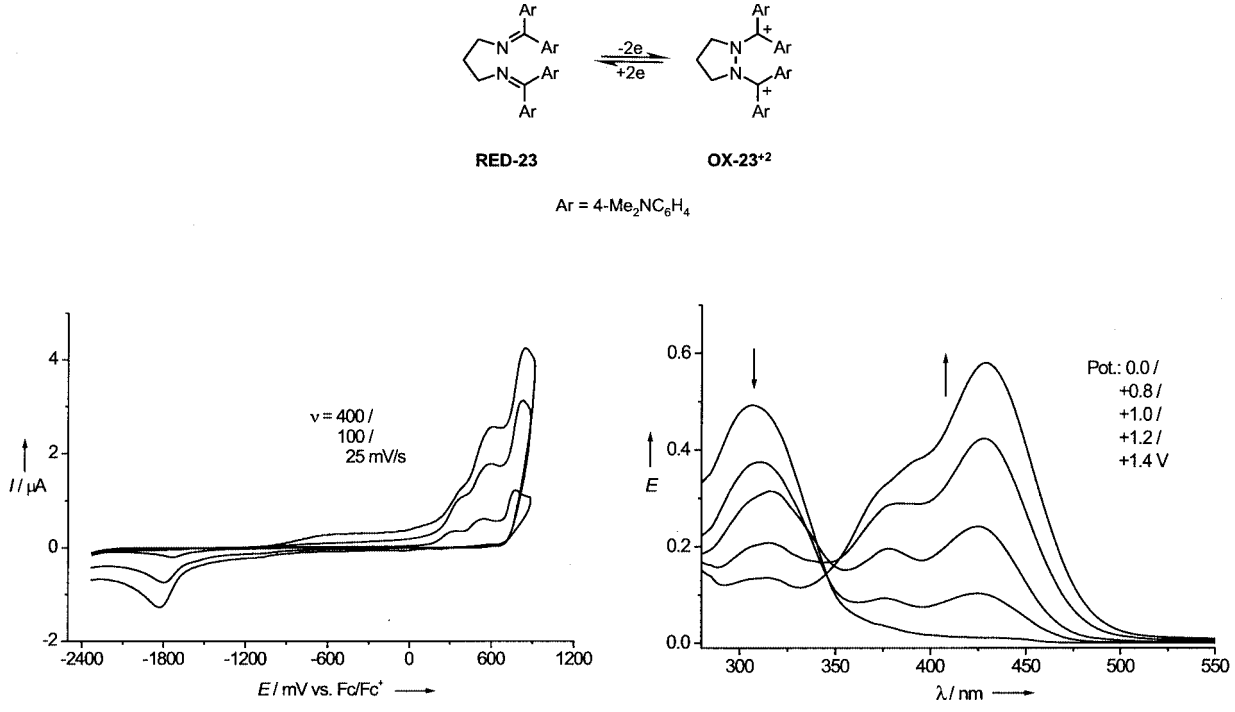

Figure 8. Cyclic voltammogram (CV) and spectroelectrogram (SE) of **RED-23** in benzonitrile

suitable ring size is achieved. In addition to electrochromic systems derived from the general structure of violene/cyanine hybrids,[12,18,19] type OL/CS[1] and type OS/CL represent another general structure in which the colored form consists of two closed-shell π-systems instead of the radical ions in classical organic electrochromic systems.[20] Electrochromic systems based on intramolecular "no bond/single bond" redox transformations according to Scheme 1[21] offer further applications in "molecular mechanics",[22] due to the strong changes in geometry. Since our group has now finally dissolved, others are encouraged to plow this promising new field.

Experimental Section

General Remarks: Melting points were determined on a hot-stage microscope (Fa. Reichert) and are corrected. IR: Perkin−Elmer 1420 spectrophotometer. ^{1}H and ^{13}C NMR: Bruker AC 250 (250 MHz) and Bruker (600 MHz) spectrometers; standardized by solvent signals. MS: Varian MT CH7 and Finnigan MAT 8200 spectrometers.

Electrochemical Measurements: Cyclic voltammetry (CV) was performed in a three-electrode, single-compartment cell (5 mL) with a computer-controlled EG&G PAR 273 potentiostat. CV data were obtained at a glassy carbon disk electrode with a surface of A = 0.785 mm^2. The counterelectrode consisted of a platinum wire, the reference electrode was an Ag/AgCl secondary electrode. Acetonitrile (Licrosolv, Merck) was filtered through aluminum oxide directly into the electrochemical cell. Benzonitrile was distilled prior to use. Tetrabutylammonium hexafluorophosphate puriss. (Bu_4NPF_6) was obtained from Fluka and dried in vacuo at 200 °C. All potentials were measured at 21 °C and internally referenced to ferrocene-ferricenium couple. General procedure for CV measurements: A solution of 0.1 M Bu_4NPF_6 in acetonitrile or benzonitrile was deoxygenated with dry argon for 15 min. The corresponding compounds were characterized at a concentration of ca. 1 mM with a scan rate of v = 100 mV·s^{-1} unless otherwise stated.

Spectroelectrochemical Measurements (SEs): SEs were recorded with a Perkin−Elmer Lambda 19 spectrophotometer in conjunction with an EG&G PAR potentiostat, model 363. All optical measurements were carried out at 21 °C in a thin-layer electrochemical cell (distance working electrode/light conductor: 60 μm) according to Salbeck,[23] incorporating a polished platinum disk electrode (ϕ 6 mm) as working electrode, an Ag/AgCl wire as reference electrode, and a platinum sheet as counterelectrode. Spectra were recorded in a reflection modus at the platinum electrode with the aid of a y-type optical fiber bundle.

General Procedure for SE Measurements: The potentials stated in the figures were applied to a solution of the substrate (ca. 0.1 mM) in acetonitrile or benzonitrile containing Bu_4NPF_6 (0.1 mM) and the spectra recorded after equilibration was observed. The potentials did not match those from CV measurements. Differences of up to 300 mV occurred, due to the actual geometry of the electrochemical cell used in the specific experiment.

4,4′-Bis(dimethylamino)benzophenone Hydrazone (Michler's Ketone Hydrazone, 6): In an improvement of the procedure in ref.[7], Michler's ketone (30.0 g, 0.11 mol), hydrazine (47.0 g, 87% in water, 0.78 mol), and ethanol (20 mL) were heated to 200 °C in an autoclave (glass, applicable to 10 bar) for 24 h. On slow cooling and stirring, crystals deposited and were separated and washed with ice-cold ethanol (20 mL). 24.8 g (80%) pure **6**, m.p. 150−151 °C (ref.[7] m.p. 150 °C). ^{1}H NMR (200 MHz, $CDCl_3$): δ = 2.96 (s, 6 H, NCH_3), 3.02 (s, 6 H, NCH_3), 4.81 (br. s, 2 H, NH), 6.64, 6.80, 7.21, 7.40 (AA′BB′ systems, J = 9.0 Hz, 8 H, ArH). ^{13}C NMR (50 MHz, $CDCl_3$): δ = 40.3, 40.4, 111.8, 112.4, 120.4, 127.4, 128.1, 130.0, 150.5. IR (KBr): $\tilde{\nu}$ = 3325 (m), 1625 (s), 1550 (w), 1545 (s), 1485 (w), 1445 (m), 1350 (s), 1290 (w), 1225 (m), 1180 (s), 1170 (m), 1160 (m), 1125 (w), 1065 (w) cm^{-1}.

General Procedure for Bis(azines) RED-8, RED-13, RED-16, RED-17: Solutions of hydrazone **6** and the diones **7**, **12**, **14**, or **15** in dichloromethane (10 mL) were stirred for 2 h in the presence of acetic acid (10 mg) and molecular sieves (4 Å, 50 mg). The filtered solution was extracted with satd. sodium hydrogen carbonate solution and dried with sodium sulfate. After evaporation of the solvent, the residue was treated with petroleum ether to yield the bis(azines) as colored powders.

Bis(azine) RED-8: Hydrazone **6** (0.80 g, 2.85 mmol) and cyclooctane-1,5-dione[20] (**7**, 0.20 g, 1.43 mmol) afforded **RED-8** (0.70 g, 73%) as a pale yellow powder, m.p. 209−210 °C. Recrystallization from acetonitrile (10 mL) yielded yellow crystals (0.3 g), m.p. 212−214 °C, consisting of only one isomer (^{1}H NMR, C_6D_6). After the NMR solution had been kept at 20−25 °C for 0.5 h, the signals of a second isomer appeared (the ratio of the two isomers was determined by integration of the *N*-methyl signals in their ^{1}H NMR spectra; ratio major isomer/minor isomer = 9:1). ^{1}H NMR (600 MHz, C_6D_6): major isomer: δ = 2.00 (m, 4 H, CH_2), 2.42 (m, 4 H, CH_2), 2.75 (m, 4 H, CH_2), 2.484 (s, 12 H, NCH_3), 2.486 (s, 12 H, NCH_3), 6.51, 6.60, 7.61, 8.06 (AA′BB′ systems, J = 9.0 Hz, 16 H, ArH); minor isomer: δ = 1.80 (m, 4 H, CH_2), 2.83 (m, 8 H, CH_2), 2.45 (s, 12 H, NCH_3), 2.48 (s, 12 H, NCH_3), 6.57, 6.59, 7.59, 8.11 (AA′BB′ systems, J = 9.0 Hz, 16 H, ArH). ^{13}C NMR (50 MHz, C_6D_6): both isomers: δ = 23.0, 25.1, 30.9, 31.5, 37.2, 37.8, 39.91, 39.93, 39.97, 39.98, 111.41, 111.56, 111.91, 111.99, 124.9, 125.0, 129.1, 129.3, 131.1, 131.2, 132.4, 132.8, 150.6, 150.7, 151.3, 151.6, 161.8, 162.2, 168.92, 168.99. IR (KBr): $\tilde{\nu}$ = 1610 (s), 1520 (m), 1450 (w), 1365 (m), 1330 (m), 1290 (w), 1230 (w), 1190 (m), 1170 (w), 1065 (w), 950 (w), 820 (m), 750 (w), 670 (w) cm^{-1}. MS (70 eV): m/z (%) = 668 (2) [M]$^+$, 430 (2), 404 (18), 376 (8), 347 (8), 282 (19), 266 (100), 250 (28), 223 (62), 145 (16), 120 (33). $C_{42}H_{52}N_8$ (668.4): calcd. C 75.41, H 7.83, N 16.75; found C 75.33, H 7.55, N 16.51.

Bis(azine) RED-13: Hydrazone **6** (0.44 g, 1.56 mmol) and heptane-2,6-dione[24] (**12**, 0.10 g, 0.78 mmol) yielded **RED-13** (0.36 g, 70%), yellow powder with m.p. 124−125 °C. Without exclusion of air, **RED-13** decomposed rapidly in solution. ^{1}H NMR (600 MHz, $CDCl_3$): δ = 1.73 (m, 2 H, CH_2), 2.19 (m, 4 H, CH_2), 2.95 (s, 3 H, CH_3), 2.96 (s, 12 H, NCH_3), 2.97 (s, 3 H, CH_3), 2.99 (s, 12 H, NCH_3), 6.64, 6.67, 7.16, 7.59 (AA′BB′ systems, J = 9.0 Hz, 16 H, ArH). ^{13}C NMR (50 MHz, $CDCl_3$): δ = 17.7, 23.2, 38.2, 40.2, 40.3, 110.8, 111.3, 123.3, 127.4, 130.0, 131.1, 150.3, 151.2, 159.0, 161.8. IR (KBr): $\tilde{\nu}$ = 1605 (s), 1560 (w), 1515 (s), 1470 (w), 1435 (m), 1350 (s), 1320 (m), 1220 (m), 1180 (s), 1160 (m), 1120 (w), 1050 (w), 940 (m), 820 (s), 740 (w) cm^{-1}. $C_{41}H_{52}N_8$ (656.9): calcd. C 74.96, H 7.98, N 17.06; found C 74.62, H 7.69, N 16.88.

Bis(azine) RED-16: Compound **RED-16** (93 mg, 63%) was obtained from **6** (124 mg, 0.44 mmol) and diketone **14**[15] (38 mg, 0.22 mmol), as a beige powder with m.p. 243−245 °C, consisting of a mixture of two isomers (ratio 2:1, ^{1}H NMR). ^{1}H NMR (600 MHz, $CDCl_3$): major isomer: δ = 2.81 (s, 6 H, NCH_3), 2.86 (s, 6 H, NCH_3), 2.99 (s, 6 H, NCH_3), 3.00 (s, 6 H, NCH_3), 7.17, 7.19, 7.58, 7.66 (AA′BB′ systems, J = 9.0 Hz, 16 H, ArH); minor isomer: δ = 2.94 (s, 6 H, NCH_3), 2.95 (s, 6 H, NCH_3), 2.96 (s, 6 H, NCH_3), 2.97 (s, 6 H, NCH_3), 7.18, 7.19, 7.50, 7.52 (AA′BB′ systems, J = 8.9 Hz, 16 H, ArH); aliphatic proton resonances of both isomers: δ = 1.61, 1.91, 2.65, 2.69, 2.85−3.06, 3.07, 3.10, 3.27, 3.96, 4.01−4.07; aromatic proton resonances of both isomers: δ = 6.58−6.67. ^{13}C NMR (151 MHz, $CDCl_3$): major isomer: δ = 37.4, 38.7, 40.1, 40.2, 40.34, 40.36, 40.9, 42.9, 45.3, 45.7, 46.4, 51.3, 110.9, 110.2, 111.2, 111.3, 123.0, 123.1, 127.6, 127.7, 130.5, 130.6, 132.1, 132.4, 150.4, 150.5, 163.6, 164.2; minor isomer: δ = 37.1, 38.6, 40.0, 40.2, 40.34, 40.36, 40.7, 42.9, 45.5, 45.6, 46.1, 51.5, 110.2, 110.9, 111.31, 111.35, 123.2, 123.3, 127.6, 127.8, 130.5, 130.6, 132.1, 132.3, 151.3, 151.4, 172.4, 173.5. IR (KBr): $\tilde{\nu}$ = 1630 (m), 1605 (s), 1560 (m), 1525 (m, shoulder), 1510 (s), 1470 (w), 1440 (m), 1420 (w), 1400 (w), 1350 (s), 1320 (s), 1280 (w), 1220

(m), 1180 (s), 1160 (m), 1145 (m, shoulder), 1115 (w), 1050 (w), 940 (m), 920 (w, shoulder), 820 (m), 805 (m), 740 (w), 735 (w, shoulder), 665 (w) cm^{-1}. $C_{45}H_{50}N_8$ (702.9): calcd. C 76.89, H 7.17, N 15.94; found C 76.22, H 6.82, N 15.21.

Bis(azine) RED-17: Hydrazone **6** (311 mg, 110 mmol) and diketone **15**[25] (110 mg, 0.55 mmol) yielded **RED-17** (280 mg, 70%) as a beige powder with m.p. 205−208 °C, consisting of a mixture of two isomers (ratio 2:1, ^1H NMR). ^1H NMR (600 MHz, $CDCl_3$): major isomer: δ = 2.82 (s, 6 H, NCH_3), 2.86 (s, 6 H, NCH_3), 2.99 (s, 6 H, NCH_3), 3.02 (s, 6 H, NCH_3), 7.58, 7.67 (AA′BB′ systems, J = 8.9 Hz, 16 H, ArH); minor isomer: δ = 2.94 (s, 6 H, NCH_3), 2.95 (s, 6 H, NCH_3), 2.96 (s, 6 H, NCH_3), 2.97 (s, 6 H, NCH_3), 7.50, 7.52 (AA′BB′ systems, J = 8.9 Hz, 16 H, ArH); aliphatic proton resonances of both isomers: δ = 0.50, 0.62, 1.98, 2.04, 2.07, 2.12, 3.06, 3.29−3.40, 4.07, 4.13, 4.19, 4.27; aromatic proton resonances of both isomers: δ = 6.58−6.71, 7.17−7.21. ^{13}C NMR (151 MHz, $CDCl_3$): major isomer: δ = 4.6, 5.2, 35.2, 38.0, 40.1, 40.2, 41.2, 43.5, 46.3, 51.2, 51.80, 51.82, 52.4, 110.92, 110.98, 111.2, 111.3, 123.1, 123.2, 127.6, 127.7, 130.5, 130.6, 132.1, 132.4, 150.35, 150.39, 151.3, 151.4, 163.6, 164.3, 172.5, 173.6; minor isomer: δ = 4.71, 5.27, 35.2, 37.6, 40.34, 40.36, 41.1, 43.8, 46.1, 51.2, 51.6, 51.8, 52.0, 110.92, 110.98, 111.30, 111.37, 123.2, 123.3, 127.7, 127.8, 130.5, 130.6, 132.3, 132.4, 133.0, 150.50, 150.54, 151.0, 151.3, 163.4, 163.7, 172.2, 173.2. IR (KBr): ṽ = 1635 (m), 1605 (s), 1570 (m), 1535 (m, shoulder), 1520 (s), 1480 (w), 1445 (m), 1425 (w), 1410 (w), 1365 (s), 1360 (s), 1330 (s), 1290 (m), 1230 (m), 1190 (s), 1170 (m), 1155 (w, shoulder), 1125 (w), 1050 (w), 940 (m), 925 (w), 825 (s), 805 (w, shoulder), 770 (w), 750 (w), 745 (w), 685 (w), 670 (w) cm^{-1}. $C_{47}H_{52}N_8$ (728.99): calcd. C 77.44, H 7.17, N 15.37; found C 76.57, H 6.92, N 15.23.

Bis(imine) RED-22: A solution of chloride **18**[16] (349 mg, 1.08 mmol) and triethylamine (275 mg, 2.71 mmol) was slowly added to a stirred solution of 2,2′-diaminobiphenyl[26] (**19**, 100 mg, 0.54 mmol) in dichloromethane (2 mL) at room temperature. After stirring at 20 °C for 2 h, the mixture was extracted twice with satd. sodium hydrogen carbonate solution (10 mL) and dried (Na_2SO_4), and the solvents were evaporated. On stirring the red oily residue (320 mg) overnight with ethyl acetate/hexane (4:1, 10 mL), an orange powder precipitated. This product was then stirred with diethyl ether (3 × 10 mL, 1 h) to yield **RED-22** (230 mg, 65%) as an orange solid with m.p. 254−250 °C. ^1H NMR (600 MHz, $CDCl_3$): δ = 2.86 (s, 12 H, NCH_3), 2.97 (s, 12 H, NCH_3), 6.29, 6.63, 6.77, 7.70 (AA′BB′ systems, J = 8.8 Hz, 16 H, ArH), 6.66−6.73 (m, 6 H, ArH), 6.94−6.96 (m, 2 H, ArH). ^{13}C NMR (150 MHz, $CDCl_3$): δ = 40.1, 40.2, 110.6, 111.0, 121.3, 121.6, 124.7, 126.4, 129.8, 131.2, 131.4, 131.7, 131.9, 149.9, 150.0, 151.5, 166.6. IR (KBr): ṽ = 1610 (s), 1580 (s), 1550 (m), 1525 (w), 1485 (w), 1445 (w), 1435 (w), 1365 (m), 1345 (m), 1320 (m), 1285 (w), 1230 (w), 1190 (m), 1170 (m), 1150 (w), 1065 (w), 950 (m), 825 (m), 820 (m), 785 (w), 765 (m), 755 (m), 725 (w), 680 (w) cm^{-1}. $C_{44}H_{48}N_6$ (660.9): calcd. C 79.96, H 7.32, N 12.72; found C 79.49, H 7.00, N 12.45.

Bis(imine) RED-23: A mixture of 1,3-diaminopropane (**20**, 68 mg, 0.92 mmol), chloride **18** (741 mg, 2.29 mmol), and sodium hydride suspension (550 mg, 23 mmol) in THF (30 mL) was stirred at room temperature until evolution of gas ceased (ca. 4 h). After evaporation of the filtered solution, a yellow oil remained, and was treated as described for **RED-22** to yield **RED-23** (185 mg, 35%) as a yellow powder of m.p. 176−177 °C. ^1H NMR (200 MHz, $CDCl_3$): δ = 2.03 (quint, J = 7.0 Hz, 2 H, CH_2), 2.96 (s, 12 H, NCH_3), 2.99 (s, 12 H, NCH_3), 3.46 (t, J = 7.0 Hz, 4 H, CH_2), 6.59, 6.70, 7.02, 7.43 (AA′BB′ systems, J = 9.0 Hz, 16 H, ArH). ^{13}C NMR (51 MHz, $CDCl_3$): δ = 32.8, 40.2, 40.3, 50.7, 110.6, 111.2, 111.5, 130.0, 130.9, 132.2, 150.6, 152.0. IR (KBr): ṽ = 1600 (s), 1550 (m), 1510 (s), 1470 (m), 1435 (m), 1420 (w, shoulder), 1355 (s), 1300 (m), 1215 (m), 1185 (m), 1150 (m), 1145 (w), 1115 (w), 1050 (w), 935 (m), 810 (s), 745 (w), 735 (w), 675 (w) cm^{-1}. $C_{37}H_{46}N_6$ (574.81): calcd. C 77.31, H 8.07, N 14.62; found C 76.98, H 7.75, N 14.04.

Bis(imine) RED-24: The procedure as used for **RED-23**, but with 1,4-diaminobutane (**21**, 31.7 mg, 0.36 mmol), dichloride **18** (236 mg, 0.73 mmol), and sodium hydride (105 mg, 4.37 mmol), afforded **RED-24** (150 mg, 35%) as a yellow powder, decomposing at 240 °C. ^1H NMR (200 MHz, $CDCl_3$): δ = 1.68 (m, 4 H, CH_2), 3.39 (m, 4 H, CH_2), 2.96 (s, 12 H, NCH_3), 3.00 (s, 12 H, NCH_3), 6.60, 6.72, 7.01, 7.47 (AA′BB′ systems, J = 8.9 Hz, 16 H, ArH). ^{13}C NMR (51 MHz, $CDCl_3$): δ = 29.7, 53.6, 40.3, 111.2, 111.5, 116.2, 125.3, 129.4, 129.8, 150.1, 151.3. IR (KBr): ṽ = 1610 (s), 1520 (s), 1445 (m), 1355 (m), 1325 (m), 1185 (w), 1165 (w), 1135 (w), 1035 (w), 950 (w), 815 (w) cm^{-1}. $C_{38}H_{48}N_6$ (588.84): calcd. C 77.51, H 8.22, N 14.27; found C 77.02, H 7.88, N 14.55.

X-ray Crystallography: X-ray diffraction experiments were carried out with a Bruker Smart Apex diffractometer (D8 Goniometer); scan mode ω; software SHELXTL-NT V5.1[27,28] Crystal data and experimental details for **RED-8** are summarized in Table 3. CCDC-166669 contains the supplementary crystallographic data for this paper. These data can be obtained free of charge at www.ccdc.cam.ac.uk/conts/retrieving.html or from the Cambridge Crystallographic Data Centre, 12, Union Road, Cambridge CB2 1EZ, UK [Fax: (internat.) + 44-1223/336-033; E-mail: deposit@ccdc.cam.ac.uk].

Computational Procedure: The geometries of the studied compounds were optimized by PM3 and AM1 semiempirical methods as implemented in the HyperChem 6.03 software package.[29] In both cases, the Polak−Ribiere algorithm was used for the optimization with an SCF convergence limit of $1 \cdot 10^{-6}$; the gradient norm achieved in all calculations was less than 0.001 $kcal \cdot mol^{-1} \cdot Å^{-1}$.

Table 3. Crystal data and experimental details for **RED-8**

Compound	**RED-8**
Empirical formula	$C_{42}H_{52}N_8$
M_r	668.92
Crystal size [mm]	0.4×0.3×0.2
Space group	$P2_1/c$
a [pm]	1633.72(8)
b [pm]	987.18(5)
c [pm]	2282.61(11)
β [°]	91.9420(10)
V [nm^3]	3679.2(3)
Z	4
$\rho_{calcd.}$ [Mgm^{-3}]	1.208
μ [mm^{-1}]	0.073
F(000)	1440
Θ range [°]	1.25−23.26
No. of refln. measd.	22954
No. of unique refln.	5273
R(int)	0.0464
Data/restraints/param.	5273/41/478
Goodness-of-fit on F^2	1.243
$R1$ [$I > 2\sigma(I)$]	0.0998
$wR2$	0.2034
$g1/g2$	0.0530/4.6405
Largest diff. peak/hole [e nm^{-3}]	284/−198

Restricted Hartree−Fock (RHF) formalism was employed for all closed-shell structures (**RED-8** and **OX-8**$^{2+}$), whereas spin-unrestricted Hartree−Fock (UHF) formalism was applied for the diradical dication **OX-8**$^{2+\cdot\cdot}$ (8), and a comparative UHF calculation was also performed for the closed-shell bicyclic structure **OX-8**$^{2+}$ (5/5) for adequate comparison of the energies.

Acknowledgments

Financial support by the Fonds der Chemischen Industrie, Frankfurt/Main, and the Bayer AG, Leverkusen, is very gratefully acknowledged.

[1] S. Hünig, C. A. Briehn, P. Bäuerle, A. Emge, *Chem. Eur. J.* **2001**, *7*, 2745−2757.
[2] W. Freund, S. Hünig, *J. Org. Chem.* **1987**, *52*, 2154−2161.
[3] S. Hünig, M. Horner, *J. Am. Chem. Soc.* **1977**, *99*, 6120−6122.
[4] T. Suzuki, M. Kondo, T. Nakamura, T. Fukushima, T. Miyashi, *J. Chem. Soc., Chem. Commun.* **1977**, 2325−2326.
[5] H. Weingarten, J. S. Wager, *J. Org. Chem.* **1970**, *35*, 1750−1753.
[6] T. Suzuki, T. Yoshino, J. Nishida, M. Ohkita, T. Tsuji, *J. Org. Chem.* **2000**, *65*, 5514−5521.
[7] L. Wolff, *Justus Liebigs Ann. Chem.* **1912**, *394*, 23−108.
[8] H. Tsutsui, T. Ichikawa, K. Narasaka, *Bull. Chem. Soc. Jpn.* **1999**, *72*, 1869−1878.
[9] V. A. Sauro, M. S. Workentin, *J. Org. Chem.* **2001**, *66*, 831−838.
[10] For a amore detailed discussion of such CVs, see ref.[1]
[11] E. Malamidou-Xenikaki, N. E. Alexandrou, *Liebigs Ann. Chem.* **1986**, 280−286.
[12] S. Hünig, M. Kemmer, H. Wenner, F. Barbosa, G. Gescheidt, I. F. Perepichka, P. Bäuerle, A. Emge, K. Peters, *Chem. Eur. J.* **2000**, *6*, 2618−2632.
[13] Professor Dr. A. Griesbeck, Institute of Organic Chemistry, University of Cologne (Germany), kindly provided diketones **12** and **13** for us.
[14] A. J. H. Klander, B. Zwanenburg, *Chem. Rev.* **1989**, *89*, 1035−1050.
[15] F. J. C. Martins, A. M. Viljoen, M. Coetzee, L. Fourie, P. L. Wessels, *Tetrahedron* **1991**, *47*, 9215−9224.
[16] J. B. Conant, N. M. Bigelow, *J. Am. Chem. Soc.* **1931**, *53*, 676−690.
[17] S. F. Nelson, Y. Wang, *J. Org. Chem.* **1994**, *59*, 3082−3090; and literature cited there.
[18] S. Hünig, M. Kemmer, H. Wenner, I. F. Perepichka, P. Bäuerle, A. Emge, G. Gescheidt, *Chem. Eur. J.* **1999**, *5*, 1969−1973.
[19] S. Hünig, I. F. Perepichka, M. Kemmer, H. Wenner, P. Bäuerle, A. Emge, *Tetrahedron* **2000**, *56*, 4203−4211.
[20] S. L. Schreiber, D. B. Smith, *J. Org. Chem.* **1989**, *54*, 5994−5996.
[21] H. Berneth, S. Hünig, C. A. Briehn, S. Aldenkortt (Bayer AG), EP 1 116 767 A2; DE 100 01 031 A1.
[22] *Special Issue on Molecular Machines* (Ed.: J. F. Stoddard), *Acc. Chem. Res.* **2001**, *34*, 409−522.
[23] J. Salbeck, *J. Electroanal. Chem.* **1992**, *340*, 169.
[24] R. A. Micheli, Z. G. Hajos, N. Cohen, D. R. Parish, L. A. Portland, W. Sciamanna, M. A. Scott, P. A. Wehrli, *J. Org. Chem.* **1975**, *40*, 675−681.
[25] V. Singh, B. N. S. Raju, *Ind. J. Chem.* **1996**, *35*, 303−311.
[26] S. D. Ross, G. J. Kahan, W. A. Leach, *Org. Synth.* **1952**, *7*, 4122−4126.
[27] G. M. Sheldrick, *Acta Crystallogr., Sect. A* **1990**, *461*, 467−473.
[28] G. M. Sheldrick, *SHELXTL-NT V5.1*, Program for Crystal Structure Refinement, University of Göttingen, **1993**.
[29] *HyperChem*, Release 6.03 for Windows9x/NT/2K, Molecular Modeling System, Hypercube Inc., Gainesville, Florida, USA, **2000**.

Received November 8, 2001
[O01540]